

The Cryosphere Discussions is the access reviewed discussion forum of *The Cryosphere*

The role of radiation penetration in the energy budget of the snowpack at Summit, Greenland

P. Kuipers Munneke¹, M. R. van den Broeke¹, C. H. Reijmer¹, M. M. Helsen¹,
W. Boot¹, M. Schneebeli², and K. Steffen³

¹Institute for Marine and Atmospheric Research, Utrecht University, Utrecht, The Netherlands

²WSL Institute for Snow and Avalanche Research, Davos, Switzerland

³Cooperative Institute for Research in Environmental Sciences, University of Colorado, USA

Received: 25 Mar 2009 – Accepted: 1 April 2009 – Published: 8 April 2009

Correspondence to: P. Kuipers Munneke (p.kuipersmunneke@uu.nl)

Published by Copernicus Publications on behalf of the European Geosciences Union.

TCD

3, 277–306, 2009

Radiation penetration at Summit, Greenland

P. Kuipers Munneke et al.

Title Page

Abstract

Introduction

Conclusions

References

Tables

Figures

◀

▶

◀

▶

Back

Close

Full Screen / Esc

Printer-friendly Version

Interactive Discussion



Abstract

Measurements of the summer surface energy balance at Summit, Greenland, are presented (8 June–20 July 2007). These measurements serve as input to an energy balance model that searches for a surface temperature for which closure of all energy terms is achieved. A good agreement between observed and modeled surface temperatures was found, with an average difference of 0.45°C and an RMSE of 0.85°C . It turns out that penetration of shortwave radiation into the snowpack plays a small but important role in correctly simulating snow temperatures. After 42 days, snow temperatures in the first meter are $3.6\text{--}4.0^{\circ}\text{C}$ higher compared to a model simulation without radiation penetration. Sensitivity experiments show that these results cannot be reproduced by tuning the heat conduction process alone, by varying snow density or snow diffusivity. We compared the two-stream radiation penetration calculations with a sophisticated radiative transfer model and discuss the differences. The average diurnal cycle shows that net shortwave radiation is the largest energy source ($+61\text{ W m}^{-2}$ on average), net longwave radiation the largest energy sink (-42 W m^{-2}). On average, subsurface heat flux, sensible and latent heat fluxes are the remaining, small heat sinks (-5 , -5 and -7 W m^{-2} , respectively), although these are more important on a subdaily timescale.

1 Introduction

The energy balance at the surface of a snowpack is given by

$$SW_{\text{net}} + LW_{\text{net}} + H_{\text{sen}} + H_{\text{lat}} + \tilde{G}_s = M \quad (1)$$

where the net shortwave radiation, SW_{net} , is the sum of global shortwave radiation, SW_{\downarrow} , and reflected radiation, SW_{\uparrow} ; net longwave radiation, LW_{net} , is the sum of downwelling longwave radiation, LW_{\downarrow} , and upwelling longwave radiation, LW_{\uparrow} ; H_{sen} is the turbulent sensible heat flux, H_{lat} is turbulent latent heat flux, \tilde{G}_s is the subsurface heat flux at the surface, and M is the amount of melt energy.

TCD

3, 277–306, 2009

Radiation penetration at Summit, Greenland

P. Kuipers Munneke et al.

Title Page

Abstract

Introduction

Conclusions

References

Tables

Figures

◀

▶

◀

▶

Back

Close

Full Screen / Esc

Printer-friendly Version

Interactive Discussion



In the absence of meltwater percolation, the temperature distribution within the snow-pack is governed mainly by heat conduction, which has a diffusive nature. Close to the surface, also non-diffusive processes take place, like subsurface penetration and subsequent absorption of shortwave radiation (Colbeck, 1989b), wind pumping (Colbeck, 1989a), and latent heat transfer by subsurface water vapour transport (Albert and Shultz, 2002). The latter two processes are known to play a role at high wind speeds. Earlier studies suggested that the subsurface heat production by penetration of shortwave radiation could be significant (Schlatter, 1972), leading to a “solid-state greenhouse” (Matson and Brown, 1989), in which shortwave radiation is absorbed below the surface while longwave radiation is emitted at the surface. Later, it was shown that these studies overestimated this effect as they did not take into account the large variation of the extinction coefficient of snow with wavelength (Brandt and Warren, 1993). Hence, the latter authors concluded that subsurface heating in Antarctica must be very small. The importance of treating subsurface radiation spectrally is underlined by experimental studies on subsurface radiation fluxes, e.g. by Meirold-Mautner and Lehning (2004) at Summit. Although it was shown that radiation penetration was overestimated previously, Liston and Winther (2005) suggested that no less than 20% of the snow-covered area of Antarctica experiences subsurface melt. Since most of this meltwater refreezes locally, the effect on the mass balance of Antarctica is supposed to be small.

Although the effect was shown to be smaller than presumed before, it potentially affects the subsurface temperature distribution, since energy is transferred below the surface more efficiently than by conduction of heat from the surface layer alone. For ice, it was already demonstrated that radiation penetration plausibly explains observed vertical temperature distributions and vertical melt extent at several sites in the ablation zone of the Greenland ice sheet (Van den Broeke et al., 2008). For snow, the influence of radiation penetration on the formation of depth hoar (Alley et al., 1990) and crystal growth (Colbeck, 1989b) has been studied in detail, although the latter did not use a spectral model. Absorption of radiation below the surface leads to strong snow temper-

Radiation penetration at Summit, Greenland

P. Kuipers Munneke et al.

[Title Page](#)
[Abstract](#)
[Introduction](#)
[Conclusions](#)
[References](#)
[Tables](#)
[Figures](#)
[◀](#)
[▶](#)
[◀](#)
[▶](#)
[Back](#)
[Close](#)
[Full Screen / Esc](#)
[Printer-friendly Version](#)
[Interactive Discussion](#)


ature gradients just below the surface. For a correct simulation of the effect of radiation penetration on snow temperature, it is therefore important to use a sufficiently high resolution of the subsurface model (Dadic et al., 2008).

In this study, we present detailed and high-quality measurements of the energy budget of the snowpack during two summer months at Summit, Greenland, and show that subsurface absorption of penetrated radiation plays an important role for the temperature distribution in the snowpack. In Sects. 2 and 3, the data and energy balance model are presented; Sect. 4 discusses the results, and the paper is concluded and summarized in Sect. 5.

2 Data

In this section, we present data acquired in a period of 42 days from 8 June to 20 July 2007, during the Summit Radiation Experiment (SURE 07), performed at the Greenland Environmental Observatory at Summit (72°34' N 38°28' W, 3209 m a.s.l.), on top of the Greenland ice sheet.

A single-level automatic weather station (AWS) performed ventilated measurements of air temperature T_a , air pressure p , relative humidity RH, and wind speed u at 3.85 m above the surface. The specific humidity of air, q , is calculated from these data. Below the surface, subsurface snow temperatures $T_{sn,i}$ were measured at depths z_i using thermistor strings (0.20, 0.30, 0.50, 0.75 and 1.00 m) and thermocouples (spaced 0.02 m up to 0.10 m). AWS data were stored as 5-min averages on a Campbell CR10X datalogger.

The radiation components of the surface energy balance were measured with a separate installation equipped with high-quality sensors for long- and shortwave radiation. SW_{net} was measured with a pair of Kipp & Zonen (K&Z) CM21 pyranometers (the upward-looking one being ventilated); LW_{net} was measured using K&Z CG4 pyrgeometers (again, the upward-looking one being ventilated). The radiation data were stored as 1-min averages.

Radiation penetration at Summit, Greenland

P. Kuipers Munneke et al.

Title Page

Abstract

Introduction

Conclusions

References

Tables

Figures

◀

▶

◀

▶

Back

Close

Full Screen / Esc

Printer-friendly Version

Interactive Discussion



The upward-looking pyranometer regularly suffered from rime accretion during clear nights, which was removed manually every morning around 7:15 a.m. local time (09:15 GMT). SW_{\downarrow} data suspected to be corrupted by rime were replaced by parameterized data by linearly interpolating the albedo during the period of the data gap and using SW_{\uparrow} .

We compared the K&Z CG4 LW_{net} measurements with data acquired by Eppley Precision Infrared Radiometers (PIR) at the nearby candidate-BSRN radiation station (Baseline Surface Radiation Network, Ohmura et al., 1998). It was found that the CG4 LW_{\uparrow} measurements were systematically overestimated (3.5 W m^{-2} on average, peaking at $5\text{--}7 \text{ W m}^{-2}$ during daytime). Contrary to the BSRN measurements, the CG4 sensor measuring LW_{\uparrow} was not ventilated and its measurements were affected by window heating, i.e. heating of the sensor dome by reflected solar radiation. Since the thermal conduction between the dome and the thermopile measuring sensor housing temperature is near-perfect, the thermopile gets too warm and the calculated LW -fluxes too high. Window heating is less of a problem for the ventilated upward-facing CG4 (1.9 W m^{-2} difference with the Eppley PIR on average), but the BSRN Eppley PIR LW_{\downarrow} measurements are preferred as they are shielded from direct solar radiation. Comparison of the SW -fluxes with those from the BSRN site showed that our measurements have less scatter (presumably due to regular removal of accreted rime). In the remainder of this manuscript, we will therefore use the K&Z CM21 SW -fluxes from our setup and the Eppley PIR LW -fluxes from the candidate-BSRN station.

The sensible heat flux was measured directly with a Campbell CSAT3 sonic anemometer at a frequency of 20 Hz, and 5 min averages were stored on a separate Campbell CR10X datalogger. The sonic anemometer was fitted with a Campbell Chromel Constantan 75 micron thermocouple for temperature measurements. $H_{\text{sen,obs}}$ can be deduced from the measurements of vertical wind velocity and potential temperature variations w' and θ' , using the flux-profile relation

$$H_{\text{sen,obs}} = \rho_a c_p (\overline{w'\theta'})_{z_{\text{son}}}, \quad (2)$$

Radiation penetration at Summit, Greenland

P. Kuipers Munneke et al.

Title Page

Abstract

Introduction

Conclusions

References

Tables

Figures

◀

▶

◀

▶

Back

Close

Full Screen / Esc

Printer-friendly Version

Interactive Discussion



where ρ_a is the density of air, c_p the specific heat capacity of dry air, and z_{son} the sonic anemometer measurement height.

The latent heat flux was not measured directly, but rather computed using the bulk aerodynamic method as explained in Sect. 3.

3 The energy balance model

For the calculation of the energy budget of the snowpack, the model by Van den Broeke et al. (2005) was used (see also Van As et al., 2005; Giesen et al., 2008). The model calculates the energy fluxes of a skin layer without heat capacity, it employs the bulk aerodynamic method for turbulent fluxes (see Sect. 3.1), and it calculates the subsurface temperature profile using the one-dimensional heat-transfer equation (Sect. 3.3). Using SW_{net} , LW_{\downarrow} and the AWS measurements as input, the energy balance in Eq. (1) is solved iteratively in order to find a value for T_s for which the energy budget is closed. As we will see later, this iterative procedure makes the model very robust, and less susceptible to errors in input data: since all fluxes are interrelated, and a change in T_s has opposing effects on different fluxes, errors in the input are strongly damped. This was also demonstrated in an error analysis by Van As et al. (2005). The model has a time step of 1 min.

3.1 Turbulent fluxes

In the energy balance model, the turbulent fluxes are calculated using

$$H_{\text{sen}} = \rho_a c_p u_* \theta_* \quad (3)$$

$$H_{\text{lat}} = \rho_a L_{v,s} u_* q_* \quad (4)$$

Title Page

Abstract

Introduction

Conclusions

References

Tables

Figures

◀

▶

◀

▶

Back

Close

Full Screen / Esc

Printer-friendly Version

Interactive Discussion



Radiation penetration
at Summit, Greenland

P. Kuipers Munneke et al.

Title Page

Abstract

Introduction

Conclusions

References

Tables

Figures

◀

▶

◀

▶

Back

Close

Full Screen / Esc

Printer-friendly Version

Interactive Discussion



where $L_{v,s}$ is latent heat of vapourization or sublimation, depending on the surface temperature T_s . The surface friction velocity u_* , and the turbulent scaling parameters for temperature θ_* and specific humidity q_* , are computed using the bulk method – a method that exploits Monin-Obukhov similarity theory for wind, temperature and moist profiles in the surface layer, and the following assumptions at the surface: at the surface roughness length for momentum $z_{0,u}$, wind velocity $u(z_{0,u})=0$; at roughness length for temperature $z_{0,T}$, air temperature $T_a(z_{0,T})=T_s$; and at roughness length for moisture $z_{0,q}$, the air is saturated: $q(z_{0,q})=q_{\text{sat}}(z_{0,q})$. With the Monin-Obukhov length L ,

$$L = \frac{u_*^2}{\kappa g / \theta [\theta_* + 0.62 \theta q_*]}, \quad (5)$$

u_* , θ_* and q_* can be expressed using measurements of u , T_a and q at measurement levels z_u , z_T and z_q :

$$u_* = \frac{\kappa u(z_u)}{\ln\left(\frac{z_u}{z_{0,u}}\right) - \Psi_m\left(\frac{z_u}{L}\right) + \Psi_m\left(\frac{z_{0,u}}{L}\right)} \quad (6)$$

$$\theta_* = \frac{\kappa (T_a(z_T) - T_s)}{\ln\left(\frac{z_T}{z_{0,T}}\right) - \Psi_h\left(\frac{z_T}{L}\right) + \Psi_h\left(\frac{z_{0,T}}{L}\right)} \quad (7)$$

$$q_* = \frac{\kappa (q(z_q) - q_{\text{sat}}(z_{0,q}))}{\ln\left(\frac{z_q}{z_{0,q}}\right) - \Psi_h\left(\frac{z_q}{L}\right) + \Psi_h\left(\frac{z_{0,q}}{L}\right)}. \quad (8)$$

In the above equations, $\kappa=0.4$ is the Von Kármán constant; $\Psi_{m,h}$ are vertically-integrated stability correction functions taken from Holtslag and de Bruin (1988) for

stable conditions and Dyer (1974) for unstable conditions (which occur regularly during daytime at Summit – Cullen and Steffen, 2001; Cullen et al., 2007). Roughness length for momentum, $z_{0,u}$, is taken constant at 3.8×10^{-4} m, derived from sonic anemometer measurements. Values for $z_{0,T}$ and $z_{0,q}$ are calculated following Andreas (1987). Since u_* (and θ_* and q_*) requires the calculation of L , which is in turn dependent on u_* (and θ_* and q_*), the turbulent fluxes are solved iteratively.

3.2 Radiation penetration

The model includes a module to calculate subsurface radiation penetration of short-wave radiation following the method presented by (Brandt and Warren, 1993). The model is identical to the one used in Van den Broeke et al. (2008). This module employs the two-stream approach from Schlatter (1972), giving analytical functions for attenuation of shortwave radiation *per wavelength*. The module calculates radiation in 118 wavelength bands covering the solar spectrum, and uses Mie scattering coefficients derived from Warren (1984), updated with values from Warren et al. (2006) for the UV and visible wavelength range. The two-stream analytical functions require a constant snow density $\rho_{sn,rp}$ and effective snow grain radius r_e . The grid spacing for the radiation penetration calculations is 0.001 m. Results on this grid are interpolated onto the 0.01 m grid used for the subsurface calculations (see Sect. 3.3). Increasing the grid resolution any further did not affect the results.

Energy released by radiation penetration in the snowpack is added to the appropriate subsurface model layers, and the total amount of penetrated radiation Q is subtracted from the surface skin layer. Equation (1), which is valid for the surface layer, formally becomes

$$SW_{\text{net}} + LW_{\text{net}} + H_{\text{sen}} + H_{\text{lat}} + G_s - Q = M \quad (9)$$

For an infinitesimally thin surface layer, $SW_{\text{net}}=Q$ and these terms would cancel for the surface layer. Because of the discrete nature of the model numerics however, the surface layer energy budget retains the shape of Eq. (9).

Title Page

Abstract

Introduction

Conclusions

References

Tables

Figures

◀

▶

◀

▶

Back

Close

Full Screen / Esc

Printer-friendly Version

Interactive Discussion



The hypothesized effect of incorporating radiation penetration is that energy is released below the surface, enabling a more rapid warming of the snowpack.

3.3 Subsurface flux

To obtain the subsurface heat flux G , a subsurface module is included in the model, which calculates the one-dimensional heat-transfer equation on a 0.01 m grid up to a depth of 20 m, beyond which G is assumed to be zero. The model results are insensitive to grid size smaller than 0.01 m. It was already pointed out by Dadic et al. (2008) that modeling of subsurface processes should be done at a sufficiently high resolution, as the temperature gradient attains large values. The snow density profile, $\rho_{sn}(z)$ is prescribed using measurements from several snow pits, and thus decoupled from the constant density required for the radiation penetration calculations. In each snow pit, we collected one pair of density profiles, spaced about 0.30 apart to account for horizontal variations and to reduce the measurement error. In total, 7 pairs of density profiles have been collected with an approximate resolution of 0.02 m up to a depth of 1.0 m, which were interpolated in time to account for temporal variations, and interpolated onto the 0.01 m subsurface grid. Below 1.0 m, density is taken constant at 400 kg m^{-3} .

Thermal conductivity of snow, k_{sn} , is prescribed as a function of $\rho_{sn}(z)$ (in kg m^{-3}), following Anderson (1976):

$$k_{sn} = 0.021 + 2.5 \left(\frac{\rho_{sn}}{1000} \right)^2 \quad (10)$$

The specific heat capacity of ice, $c_{p,ice}$, is a function of $T_{sn}(z)$. The vertical snow temperature profile was initialized using measurements typical for June at Summit (Hoch, 2005), scaled in the uppermost meter with our own measurements of T_{sn} .

The subsurface heat flux at the surface is denoted as G_s , and calculated using the model temperature gradient at the surface. To compare our energy budget calculations

Radiation penetration at Summit, Greenland

P. Kuipers Munneke et al.

Title Page

Abstract

Introduction

Conclusions

References

Tables

Figures

◀

▶

◀

▶

Back

Close

Full Screen / Esc

Printer-friendly Version

Interactive Discussion



with previous studies (Cullen and Steffen, 2001; Hoch, 2005) that did not explicitly distinguish between subsurface heat fluxes by diffusion and subsurface radiation penetration, we will present their combined effects as \tilde{G}_s using model snow temperatures (Hoch, 2005):

$$\tilde{G}_s = - \sum_{j=1}^{n-1} \frac{\Delta T_{sn}(z_j)/\Delta t + \Delta T_{sn}(z_{j+1})/\Delta t}{2} \cdot c_{p,ice,j} \cdot \rho_{sn,j} \cdot (z_j - z_{j+1}) \quad (11)$$

- 5 The temperatures at the subsurface grid are used, and at $z=0$ the observed $T_{s,obs}$ is prescribed, making $n=2001$. By calculating \tilde{G}_s in this way, the snowpack is regarded as a box containing a certain amount of heat, which is closed at the bottom (no heat exchange at the lower boundary) – the subsurface heat flux at the surface is thus assumed to equal the rate of change of the total heat storage in the snowpack, whether
10 caused by heat diffusion or subsurface radiation absorption. In the terminology of the equations presented above:

$$\tilde{G}_s = G_s - Q \quad (12)$$

assuming that other subsurface heat sources or sinks (e.g. wind pumping or water vapour transport) are negligible. In that case, \tilde{G}_s is the same quantity as in Eq. (1).

4 Results and comparison with measurement data

- 15 As described before, the AWS measurements, as well as the measurements of SW_{net} and LW_1 , drive the energy balance model. Its performance can be assessed by means of three criteria:

1. Calculated surface temperature $T_{s,mod}$ and observed surface temperature, $T_{s,obs}$, derived from LW_1 measurements, should be in good agreement

Title Page

Abstract

Introduction

Conclusions

References

Tables

Figures

◀

▶

◀

▶

Back

Close

Full Screen / Esc

Printer-friendly Version

Interactive Discussion



2. Calculated H_{sen} and the directly measured $H_{\text{sen,obs}}$ from the sonic anemometer should be in good agreement,
3. The evolution of subsurface temperatures $T_{\text{sn},i}$ in the model should agree with observed snow temperatures.

In this section, we present model results in the optimal setting, perform a sensitivity analysis, and demonstrate the role of radiation penetration in the energy budget of the snowpack.

4.1 Results

The optimal results of the energy balance model, determined by the best performance on the above-mentioned criteria, are shown in Fig. 1, which compares $T_{\text{s,mod}}$ and $T_{\text{s,obs}}$ (criterion 1). This calculation will be referred to as the “optimal run”.

Figure 1 shows a small, systematic bias towards high $T_{\text{s,mod}}$, with $\mu_{\Delta T_s} \equiv T_{\text{s,mod}} - T_{\text{s,obs}} = 0.45^\circ\text{C}$ and a root mean square error ($\text{RMSE}_{\Delta T_s}$) of 0.85°C . The model performs best for higher temperatures, whereas for lower temperatures, $T_{\text{s,mod}}$ tends to be too high. The discrepancy is not necessarily rooted in the model: $T_{\text{s,obs}}$ could be too low because of an offset in LW measurements, which would be typically 1.9 W m^{-2} for 0.45°C . This is well within the accuracy of the Eppley PIR pyrgeometers (10 W m^{-2}). The difference $\mu_{\Delta T_s}$ turns out to be larger for clear-sky conditions, so either the model performs less well for meteorological conditions under a clear sky, or the measurements of LW under clear sky are biased – or a combination of both.

In Fig. 2, we show a plot of modeled vs. measured sensible heat fluxes (criterion 2). The agreement is reasonable (correlation coefficient $r^2 = 0.66$). Negative values of H_{sen} are somewhat underestimated by the model whereas positive values are overestimated.

Lastly, we show the measured and modeled subsurface temperatures at 0.10, 0.50 and 0.75 m below the surface in Fig. 3a. As is clearly visible in this plot, modeled tem-

Title Page

Abstract

Introduction

Conclusions

References

Tables

Figures

◀

▶

◀

▶

Back

Close

Full Screen / Esc

Printer-friendly Version

Interactive Discussion



peratures follow the measured ones quite well, although they do not match perfectly, and especially in the first weeks of the experiment period, there is some discrepancy in the amplitude of the daily cycle at depth. We will discuss these points in Sect. 4.3.

4.2 Sensitivity experiments

5 In order to assess the sensitivity of the energy balance model to its settings and assumptions, we performed many sensitivity tests and compared the model outcome of each test with the optimal run. The results of 8 of these tests are summarized in Table 1. If $z_{0,u}$ is multiplied by 10, $T_{s,mod}$ is hardly affected. Upon division of $z_{0,u}$ by 10, $T_{s,mod}$ will deviate more from $T_{s,obs}$. Note that, by changing $z_{0,u}$ in these experiments, the roughness lengths $z_{0,T}$ and $z_{0,q}$ are also affected through the relations by Andreas (1987). Limiting the stability correction functions slightly deteriorates the results, whereas omission of the stability correction functions altogether leads to a larger disagreement between $T_{s,mod}$ and $T_{s,obs}$. The latter two tests show that applying an unlimited stability correction to the turbulent fluxes yields the best results. The robustness of the model regarding the turbulence calculations was also demonstrated by Van As et al. (2005).

Furthermore, we tested the sensitivity of model results to errors in the measured input. We varied T_{2m} by $\pm 0.1^\circ\text{C}$ to show that the model results are moderately affected. A systematic temperature measurement error of -0.7°C would be necessary to match $T_{s,mod}$ and $T_{s,obs}$, which is deemed very unlikely, since the air temperature measurements excellently agree with the independent thermocouple measurements from the sonic anemometer. Lastly, we increased snow densities ρ_{sn} and $\rho_{sn,rp}$ by 50 kg m^{-3} . We found that $T_{s,mod}$ rises by a moderate 0.04°C . On the other hand, increasing snow density does have a small impact on modeled subsurface temperatures: the increase of 50 kg m^{-3} results in a 0.66°C higher temperature at 0.75 m after 42 days, and $+0.55^\circ\text{C}$ at 0.10 m. The explanation is that both the extinction of subsurface radiation and the heat conductivity increase, enabling better conduction of

Title Page

Abstract

Introduction

Conclusions

References

Tables

Figures

◀

▶

◀

▶

Back

Close

Full Screen / Esc

Printer-friendly Version

Interactive Discussion



more absorbed radiation. However, without modeling radiation penetration, a higher density alone can never explain the observed snow temperatures. Different density-dependent formulations for thermal conductivity k_{sn} (Eq. 10) have been tried, but the results changed insignificantly. In summary, tweaking the diffusive subsurface heat flux, either by varying ρ_{sn} or k_{sn} does not lead to a match between $T_{s,mod}$ and $T_{s,obs}$.

4.3 Radiation penetration

As a part of the sensitivity study in Sect. 4.2, the radiation penetration module was switched off. The resulting effect on the subsurface temperatures is shown in Fig. 3b. As can be clearly seen, the modeled snow temperatures remain systematically lower than the measured ones. Also, the amplitude of the signal at various time scales is underestimated.

Based on the following arguments, we rule out the possibility that the discrepancy between modeled and observed T_{sn} can be explained by erroneous measurements due to radiative heating of the sensors: (1) Brandt and Warren (1993) performed a field experiment shading the snow surface, and from their findings it can be concluded that radiative heating of thermistors is by far too small at depths greater than 0.10 m to explain the discrepancy between measured and modeled snow temperatures; (2) the discrepancy persists during the night when the solar flux is small. Brandt and Warren (1993) showed in their field experiment that errors due to radiative heating of thermistors vanish a few minutes after they are shaded. We would therefore expect that night-time readings are unaffected. What we observe is quite different however: at nighttime, measured and modeled snow temperatures do not converge; (3) the discrepancy between modeled and measured temperatures does not only play a role close to the surface (0.10 m), but also at greater depth (0.50 and 0.75 m). The thermistors are shielded with a white plastic protective cover, that is highly-reflective especially for the wavelengths that do penetrate to these depths. Only for the thermocouple at 0.10 m, the amplitude of the measured T_{sn} is greater than that of the modeled T_{sn} until the beginning of July. This could be indicative of a small amount of radiative heating of

Title Page

Abstract

Introduction

Conclusions

References

Tables

Figures

◀

▶

◀

▶

Back

Close

Full Screen / Esc

Printer-friendly Version

Interactive Discussion



the thermistor; (4) other studies using exactly identical thermistor strings (Reijmer and Oerlemans, 2002; Van As et al., 2005) did not detect radiative heating of thermistors either. Rather, we propose that subsurface absorption of shortwave radiation deposits heat in snow below the surface, enabling a more rapid heating of the snowpack than by the subsurface heat flux G alone.

The amount of shortwave radiation absorbed below the surface is plotted in time in Fig. 4. Most of this radiation is absorbed close to the surface, and rapidly decreases with depth. On average, 6.3% of the incoming solar radiation is absorbed at least 0.5 cm below the surface (in the second and subsequent subsurface model layers), which equals about 37% of SW_{net} .

From a physical point of view, subsurface absorption of radiation is emphatically different from the subsurface heat flux. The first is a source term, whereas the latter is a diffusive term. This fundamental difference makes that adding a source term below the surface can successfully close the energy budget of the subsurface, whereas amending the diffusive process of heat conduction, by means of varying either k_{sn} or ρ_{sn} (Sect. 4.2), cannot. This is illustrated in Fig. 5, in which the subsurface snow temperature profile is plotted at the end of the 42-day experiment. Observed snow temperatures cannot be explained without radiation penetration, nor by increasing the snow density.

While the inclusion of subsurface absorption of radiation changes snow temperatures, it hardly affects the temperature at the surface. In Table 1, it is shown that the average difference between model and observations, $\mu_{\Delta T}$, changes insignificantly. This can be explained as follows. Almost all of the penetrated radiation is absorbed a few cm below the surface, leading to some local heating of the snow just below the surface (the “solid-state greenhouse effect” – Brandt and Warren, 1993). The temperature gradient close to the surface will decrease or even reverse, and as a result, G increases close to the surface. For the energy balance of the surface layer (see Eq. 9), it means that the diminution of SW_{net} by the amount Q is compensated for by an increase of G_s , leaving $T_{s,\text{mod}}$ almost unaltered.

Radiation penetration at Summit, Greenland

P. Kuipers Munneke et al.

Title Page

Abstract

Introduction

Conclusions

References

Tables

Figures

◀

▶

◀

▶

Back

Close

Full Screen / Esc

Printer-friendly Version

Interactive Discussion



4.4 Radiative transfer modeling of radiation penetration

The radiation penetration model by Brandt and Warren (1993) requires a constant snow grain radius and snow density. From stereographical analysis of snow samples (see below), we know that these quantities vary strongly in the top few cm of the snowpack. We therefore investigated the penetration of shortwave radiation with a doubling-adding broadband radiative transfer model (DAK – Doubling Adding KNMI), in which ice crystals are prescribed using phase scattering functions (see Kuipers Munneke et al. (2008) for a complete description, and Wang et al. (2009) for clear-sky validation). The ice crystals have the same optical constants as the snow in the two-stream model.

We compared the two-stream model with the radiative transfer model DAK, applied to the snowpack at Summit. During SURE 07, we collected several snow samples that were used to obtain r_e and density profiles in the top few cm of the snowpack. At five days between 29 June and 17 July, we fixed samples in a dyed solution of diethyl phthalate. These samples were transported to a cold laboratory in Davos, Switzerland, a surface section was cut out, and they were digitally photographed. Unbiased stereological counting of sample slices was used to get detailed profiles of r_e and snow density in the top 5 to 6 cm (Matzl and Schneebeli, 2006). Density and r_e -profiles of four of these samples are shown in Fig. 6, and were prescribed in DAK. We selected four cases of clear-sky conditions close to the time of snow sample collection. For these cases, radiosonde profiles were used to specify the atmospheric composition. Subsurface radiation absorption dQ/dz profiles calculated by DAK are shown in Fig. 7a–d (red circles), together with results from the radiation penetration model for several values of r_e and $\rho_{s,rp}=280\text{ kg m}^{-3}$ (black lines). All four plots show that radiation penetration in a snowpack with variable density and snow grain size is much more irregular than calculated with the idealized two-stream model. For the cases in Fig. 7a–c, DAK results are close to the $100\text{ }\mu\text{m}$ -profiles, while in Fig. 7d, the $350\text{ }\mu\text{m}$ profile better matches the DAK results. Which snow grain size in the Brandt and Warren (1993) model best describes the amount of absorbed radiation in the two-stream

TCD

3, 277–306, 2009

Radiation penetration at Summit, Greenland

P. Kuipers Munneke et al.

Title Page

Abstract

Introduction

Conclusions

References

Tables

Figures

◀

▶

◀

▶

Back

Close

Full Screen / Esc

Printer-friendly Version

Interactive Discussion



model depends very much on the density and snow grain size in the snow samples, and their vertical distributions.

The comparison between DAK and the two-stream model remains somewhat inconclusive. The vertical distribution of absorbed radiation is shown to be more complex than the two-stream model predicts, and results depend on snow density and snow grain size, as was shown by Brandt and Warren (1993). Measured snow grain sizes range from 100 to 500 μm , and densities from 100 to 450 kg m^{-3} , but as Fig. 7 shows, the amount of absorbed radiation is sometimes better represented by choosing $r_e=100 \mu\text{m}$ in the two-stream model, and at other times, $r_e=350 \mu\text{m}$ fits better. For the simulation of snow temperatures by the energy balance model however, only $r_e=100 \mu\text{m}$ gives correct results for the entire period. Whether this contradicts snow grain size measurements cannot be concluded unambiguously. Unfortunately, a coupling between the DAK model and the energy balance model is computationally prohibitive at present.

Both Colbeck (1989a) and Alley et al. (1990) have shown that radiation penetration facilitates the emergence of low-density snow layers (depth hoar) just below the surface, so that radiation penetration, subsurface heat flux, snow grain size and density become coupled. In our model, these couplings are all absent. Despite the above, the conclusion remains that the inclusion of subsurface absorption of solar radiation is crucial for modeling the energy budget of both the surface and the subsurface correctly.

4.5 The diurnal cycle

To conclude Sect. 4, the diurnal cycle of the components of the surface energy budget is presented, averaged over the entire measurement period. We compare our results with those reported by Hoch (2005) (H05) in June and July of 2001 and 2002.

Figure 8 shows this diurnal cycle. By far the largest source of energy at the surface is SW_{net} (+61 W m^{-2} on average; H05: +60 W m^{-2}), whereas the largest sink is LW_{net} (−42 W m^{-2} ; H05: −45 W m^{-2}). The average LW_{net} minimum value of −60 W m^{-2} occurs close to local noon (14:33 UTC), demonstrating that the temperatures of the sur-

Radiation penetration at Summit, Greenland

P. Kuipers Munneke et al.

Title Page

Abstract

Introduction

Conclusions

References

Tables

Figures

◀

▶

◀

▶

Back

Close

Full Screen / Esc

Printer-friendly Version

Interactive Discussion



face snow and the air are instantly governed by solar radiation. Due to the inland location of Summit, advection of warmer air is negligible.

The turbulent fluxes are of comparable magnitude: H_{sen} and H_{lat} amount to -5 and -7 W m^{-2} , respectively (H05: -1 W m^{-2} and -9 W m^{-2} respectively), and act as small heat sinks. Between 21:00 and 06:00 UTC, H_{sen} is a very small source of heat in a stably stratified near-surface boundary layer. Stronger mixing during daytime causes transport of heat from the surface to the air, as well as a small amount of sublimation (negative H_{lat}). On average, there is a very small amount of net deposition (fallout) or downward water vapour transport at nighttime (positive H_{lat}), although this is confined to a few nights during the measurement period. Combining the effects of diffusion from surface temperature, and radiation penetration, \tilde{G}_s is -5 W m^{-2} on average during the campaign (H05: -7 W m^{-2}), reflected in a continuous heating of the snowpack (Fig. 3). The maximum cooling rate (positive \tilde{G}_s) of the snowpack is about $+14 \text{ W m}^{-2}$ at night, and the maximum heating rate about -25 W m^{-2} during daytime.

Cullen and Steffen (2001) report higher SW_{net} ($+82 \text{ W m}^{-2}$) and lower LW_{net} (-68 W m^{-2}) values, but those were obtained in a period with dominantly clear-sky conditions.

5 Discussion and conclusions

In this study, we presented measurements and model results of the components of the energy balance of the snowpack at Summit, Greenland, during a 42-day period in June and July 2007. The energy balance model simulates observed snow surface temperatures well, although on average modeled and observed snow surface temperatures differ by 0.45°C . The energy balance model was shown to be somewhat sensitive to the prescribed surface roughness length, and to small errors in input 2-m temperatures. Furthermore, the subsurface temperatures slightly depend on the prescribed snow density profile, but the effect is small in general. It was found that observed sub-

TCD

3, 277–306, 2009

Radiation penetration at Summit, Greenland

P. Kuipers Munneke et al.

Title Page

Abstract

Introduction

Conclusions

References

Tables

Figures

◀

▶

◀

▶

Back

Close

Full Screen / Esc

Printer-friendly Version

Interactive Discussion



surface temperatures could not be reproduced without including a radiation penetration term in the energy balance model. Although observed snow grain radii in the top 5 cm range from 100 to 500 μm , subsurface temperatures could only be reconstructed using a radius of 100 μm . The use of a sophisticated radiative transfer model could not solve this possible discrepancy unambiguously, although for 3 out of 4 test cases, the 100 μm -profiles fit the radiative transfer model calculations best. Nevertheless, we argued that the inclusion of a radiation penetration term is required to close the energy budget of the snowpack satisfyingly.

A natural question that comes to mind is why subsurface absorption of shortwave radiation is apparently important at Summit, while it has not been reported to be necessary to close the energy budget at other locations, either those like Hardangerjøkulen, a small, temperate ice cap in Norway (Giesen et al., 2008), or in similar circumstances like the Antarctic Plateau (Van den Broeke et al., 2004; Van As et al., 2005). In the case of measurements on Hardangerjøkulen and melting glaciers in general, the energy fluxes from melt and internal refreezing, and the associated model uncertainties, largely exceed those of absorbed subsurface radiation or the subsurface heat flux, making it hard to assess what importance radiation penetration has in the heating of the snowpack. Before the start of the melt season at Hardangerjøkulen, the modeled snow temperatures are in fact lower than the measured ones (R. H. Giesen, personal communication, 2009), suggesting that radiation penetration has some effect on snow temperature, but this might also be attributed to some intermittent meltwater percolation and refreezing, not captured by the model. Considering that, on glaciers, snow grains can become large, snow can get wet or bare ice can appear at the surface, the magnitude of absorbed subsurface radiation will be larger than at Summit, but still smaller than melt energy fluxes. Regarding the Antarctic Plateau measurements, it could be that a combination of larger snow density (Van As et al., 2005) and smaller snow grains (Kuipers Munneke et al., 2008) makes the effect much less apparent, but this requires further study.

Acknowledgements. Fieldwork was conducted with logistical and field support from NSF/Veco

Radiation penetration at Summit, Greenland

P. Kuipers Munneke et al.

Title Page

Abstract

Introduction

Conclusions

References

Tables

Figures

◀

▶

◀

▶

Back

Close

Full Screen / Esc

Printer-friendly Version

Interactive Discussion



Polar Resources. René van Overbeeke, Henk Snellen and Carina van der Veen (IMAU) are kindly thanked for fieldwork preparation. Stephen Steiner (SLF) is thanked for cutting and photographing the snow samples.

References

- 5 Albert, M. R. and Shultz, E. F.: Snow and firn properties and air-snow transport processes at Summit, Greenland, *Atmos. Environ.*, 36, 2789–2797, 2002. 279
- Alley, R. B., Saltzman, E. S., Cuffey, K. M., and Fitzpatrick, J. J.: Summertime formation of depth hoar in Central Greenland, *Geophys. Res. Lett.*, 17, 2393–2396, 1990. 279, 292
- Anderson, E. A.: A point energy and mass balance model of a snow cover, Tech. Rep. NWS19, NOAA, 1976. 285
- 10 Andreas, E. L.: A theory for the scalar roughness and the scalar transfer coefficients over snow and sea ice, *Boundary-Layer Meteorol.*, 38, 159–184, 1987. 284, 288
- Brandt, R. E. and Warren, S. G.: Solar-heating rates and temperature profiles in Antarctic snow and ice, *J. Glaciol.*, 39, 99–110, 1993. 279, 284, 289, 290, 291, 292
- 15 Colbeck, S. C.: Air movement in snow due to windpumping, *J. Glaciol.*, 35, 209–213, 1989a. 279, 292
- Colbeck, S. C.: Snow-crystal growth with varying surface temperatures and radiation penetration, *J. Glaciol.*, 35, 23–29, 1989b. 279
- Cullen, N. J. and Steffen, K.: Unstable near-surface boundary conditions in summer on top of the Greenland ice sheet, *Geophys. Res. Lett.*, 28, 4491–4493, 2001. 284, 286, 293
- 20 Cullen, N. J., Steffen, K., and Blanken, P. D.: Nonstationarity of turbulent heat fluxes at Summit, Greenland, *Bound.-Lay. Meteorol.*, 122, 439–455, 2007. 284
- Dadic, R., Schneebeli, M., Lehning, M., Hutterli, M. A., and Ohmura, A.: Impact of the microstructure of snow on its temperature: A model validation with measurements from Summit, Greenland, *J. Geophys. Res. (D)*, 113, D14303, doi:10.1029/2007JD009562, 2008. 280, 285
- 25 Dyer, A. J.: A review of flux-profile relationships, *Bound.-Lay. Meteorol.*, 7, 363–372, 1974. 284
- Giesen, R. H., van den Broeke, M. R., Oerlemans, J., and Andreassen, L. M.: Surface energy balance in the ablation zone of Midtdalsbreen, a glacier in southern Norway: in-

TCD

3, 277–306, 2009

Radiation penetration at Summit, Greenland

P. Kuipers Munneke et al.

Title Page

Abstract

Introduction

Conclusions

References

Tables

Figures

◀

▶

◀

▶

Back

Close

Full Screen / Esc

Printer-friendly Version

Interactive Discussion



terannual variability and the effect of clouds, J. Geophys. Res. (D), 113, D21111, doi:10.1029/2008JD010390, 2008. 282, 294

Hoch, S. W.: Radiative flux divergence in the surface boundary layer. A study based on observations at Summit, Greenland, Ph.D. thesis, Swiss Federal Institute of Technology, Zürich, 2005. 285, 286, 292

Holtzlag, A. A. M. and de Bruin, H. A. R.: Applied modelling of the night-time surface energy balance over land, J. Appl. Meteorol., 27, 689–704, 1988. 283

Kuipers Munneke, P., Reijmer, C. H., van den Broeke, M. R., Stammes, P., König-Langlo, G., and Knap, W. H.: Analysis of clear-sky Antarctic snow albedo using observations and radiative transfer modeling, J. Geophys. Res. (D), 113, D17118, doi:10.1029/2007JD009653, 2008. 291, 294

Liston, G. E. and Winther, J. G.: Antarctic surface and subsurface snow and ice melt fluxes, J. Clim., 18, 1469–1481, 2005. 279

Matson, D. L. and Brown, R. H.: Solid-state greenhouses and their implications for icy satellites, Icarus, 77, 67–81, 1989. 279

Matzl, M. and Schneebeli, M.: Measuring specific surface area of snow by near-infrared photography, J. Glaciol., 52, 558–564, 2006. 291

Meirolid-Mautner, I. and Lehning, M.: Measurements and model calculations of the solar short-wave fluxes in snow on Summit, Greenland, Ann. Glaciol., 38, 279–284, 2004. 279

Ohmura, A., Dutton, E. G., Forgan, B., Fröhlich, C., Gilgen, H., Hegner, H., Heimo, A., König-Langlo, G., McArthur, B., Müller, G., Philipona, R., Pinker, R., Whitlock, C. H., Dehne, K., and Wild, M.: Baseline Surface Radiation Network (BSRN/WCRP): new precision radiometry for climate research, Bull. Am. Meteorol. Soc., 79, 2115–2136, 1998. 281

Reijmer, C. H. and Oerlemans, J.: Temporal and spatial variability of the surface energy balance in Dronning Maud Land, East Antarctica, J. Geophys. Res. (D), 107, 4759–4770, 2002. 290

Schlatter, T. W.: The local surface energy balance and subsurface temperature regime in Antarctica, J. Appl. Meteorol., 11, 1048–1062, 1972. 279, 284

Van As, D., van den Broeke, M. R., Reijmer, C. H., and van de Wal, R. S. W.: The summer surface energy balance of the high Antarctic Plateau, Boundary-Layer Meteorol., 115, 289–317, 2005. 282, 288, 290, 294

Van den Broeke, M. R., van As, D., Reijmer, C. H., and van de Wal, R. S. W.: Assessing and improving the quality of unattended radiation observations in Antarctica, J. Atm. Oc. Technol., 21, 1417–1431, 2004. 294

TCD

3, 277–306, 2009

Radiation penetration at Summit, Greenland

P. Kuipers Munneke et al.

Title Page

Abstract

Introduction

Conclusions

References

Tables

Figures

◀

▶

◀

▶

Back

Close

Full Screen / Esc

Printer-friendly Version

Interactive Discussion



- Van den Broeke, M. R., Reijmer, C. H., van As, D., van de Wal, R. S. W., and Oerlemans, J.: Seasonal cycles of Antarctic surface energy balance from automatic weather stations, *Ann. Glaciol.*, 41, 131–139, 2005. 282
- 5 van den Broeke, M., Smeets, P., Ettema, J., van der Veen, C., van de Wal, R., and Oerlemans, J.: Partitioning of melt energy and meltwater fluxes in the ablation zone of the west Greenland ice sheet, *The Cryosphere*, 2, 179–189, 2008, <http://www.the-cryosphere-discuss.net/2/179/2008/>. 279, 284
- 10 Wang, P., Knap, W. H., Kuipers Munneke, P., and Stammes, P.: Clear-sky shortwave radiative closure for the Cabauw Baseline Surface Radiation Network site, the Netherlands, *J. Geophys. Res. (D)*, in review, 2009. 291
- Warren, S. G.: Optical constants of ice from the ultraviolet to the microwave, *Appl. Opt.*, 23, 1206–1225, 1984. 284
- 15 Warren, S. G., Brandt, R. E., and Grenfell, T. C.: Visible and near-ultraviolet absorption spectrum of ice from transmission of solar radiation into snow, *Appl. Opt.*, 45, 5320–5334, 2006. 284

Radiation penetration at Summit, Greenland

P. Kuipers Munneke et al.

Title Page

Abstract

Introduction

Conclusions

References

Tables

Figures

◀

▶

◀

▶

Back

Close

Full Screen / Esc

Printer-friendly Version

Interactive Discussion



Radiation penetration at Summit, Greenland

P. Kuipers Munneke et al.

Table 1. Overview of sensitivity studies performed with the energy balance model.

Sensitivity test	$\mu_{\Delta T}$ (°C)	RMSE $_{\Delta T}$ (°C)
Optimal run	0.45	0.85
$z_{0,u} \times 10$	0.45	0.87
$z_{0,u}/10$	0.60	1.02
Limited stability correction	0.53	0.93
No stability correction	0.72	1.17
$T_a + 0.1^\circ\text{C}$	0.52	0.89
$T_a - 0.1^\circ\text{C}$	0.39	0.83
Snow density $+50 \text{ kg m}^{-3}$	0.49	0.89
No radiation penetration	0.47	1.03

[Title Page](#)
[Abstract](#)
[Introduction](#)
[Conclusions](#)
[References](#)
[Tables](#)
[Figures](#)
[I◀](#)
[▶I](#)
[◀](#)
[▶](#)
[Back](#)
[Close](#)
[Full Screen / Esc](#)
[Printer-friendly Version](#)
[Interactive Discussion](#)


Radiation penetration at Summit, Greenland

P. Kuipers Munneke et al.

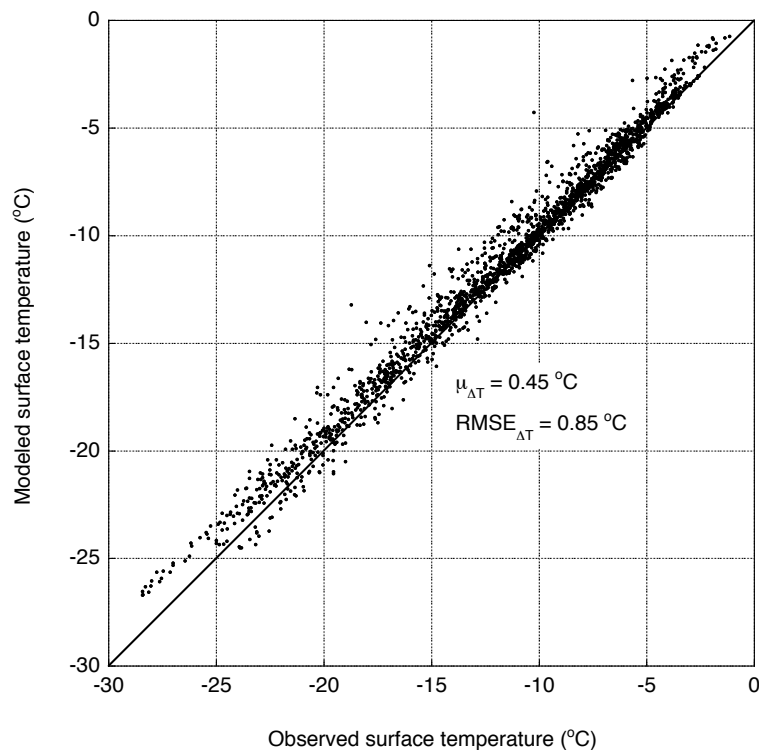


Fig. 1. $T_{s,\text{mod}}$ vs. $T_{s,\text{obs}}$ (in °C) for the optimal run. Radiation penetration is enabled, with $r_e = 100 \text{ } \mu\text{m}$, and $\rho_{sn,rp} = 280 \text{ kg m}^{-3}$. Roughness length for momentum $z_{0,u} = 3.8 \times 10^{-4} \text{ m}$.

[Title Page](#)
[Abstract](#)
[Introduction](#)
[Conclusions](#)
[References](#)
[Tables](#)
[Figures](#)
[I◀](#)
[▶I](#)
[◀](#)
[▶](#)
[Back](#)
[Close](#)
[Full Screen / Esc](#)
[Printer-friendly Version](#)
[Interactive Discussion](#)


**Radiation penetration
at Summit, Greenland**

P. Kuipers Munneke et al.

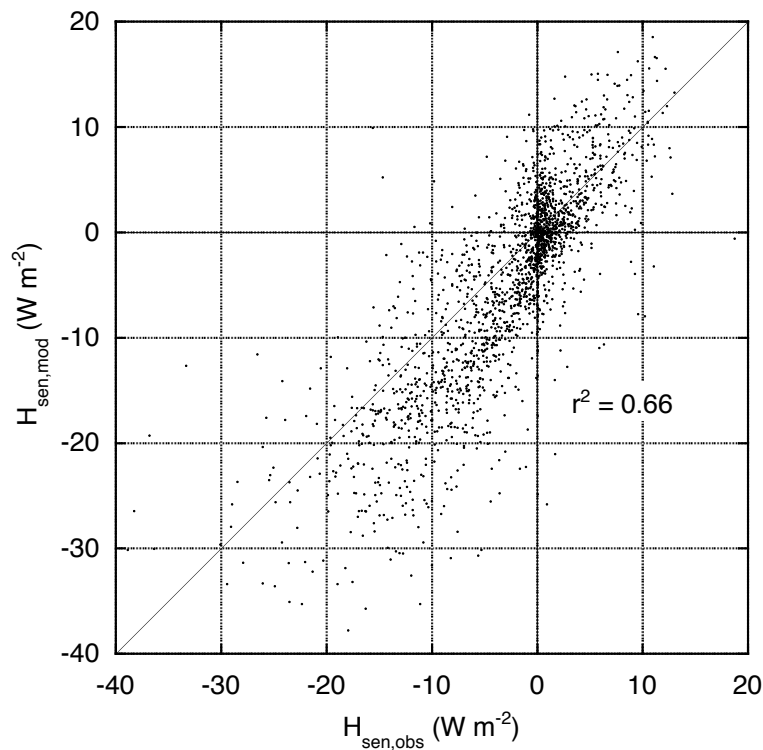


Fig. 2. $H_{\text{sen,mod}}$ vs. $H_{\text{sen,obs}}$ (in W m^{-2}) for the optimal run.

[Title Page](#)[Abstract](#)[Introduction](#)[Conclusions](#)[References](#)[Tables](#)[Figures](#)[I◀](#)[▶I](#)[◀](#)[▶](#)[Back](#)[Close](#)[Full Screen / Esc](#)[Printer-friendly Version](#)[Interactive Discussion](#)

Radiation penetration at Summit, Greenland

P. Kuipers Munneke et al.

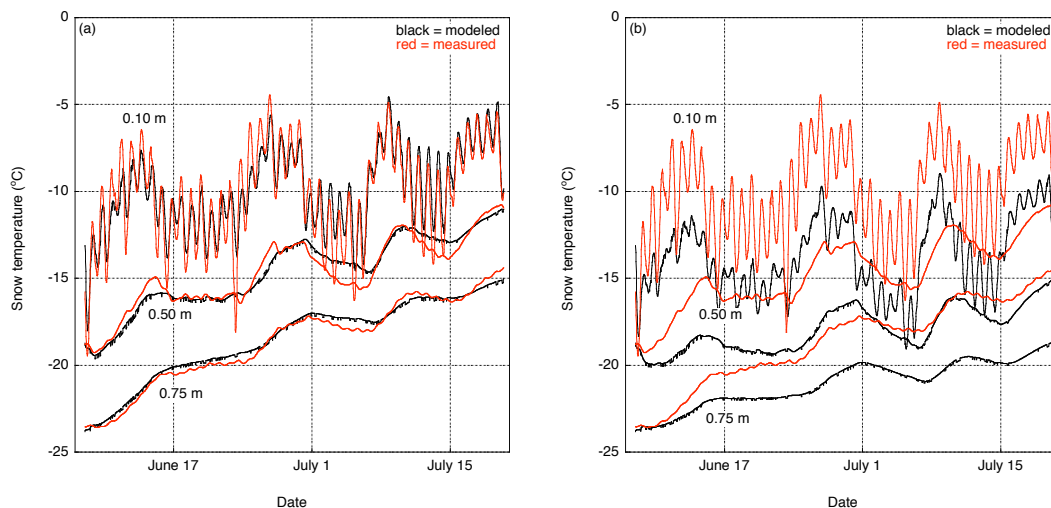


Fig. 3. Comparison between modeled (black) and observed (red) snow temperatures at 0.10 m, 0.50 m, and 0.75 m, for **(a)** the optimal run with radiation penetration, and **(b)** the run without radiation penetration, all other settings being equal.

[Title Page](#)[Abstract](#)[Introduction](#)[Conclusions](#)[References](#)[Tables](#)[Figures](#)[I◀](#)[▶I](#)[◀](#)[▶](#)[Back](#)[Close](#)[Full Screen / Esc](#)[Printer-friendly Version](#)[Interactive Discussion](#)

Radiation penetration at Summit, Greenland

P. Kuipers Munneke et al.

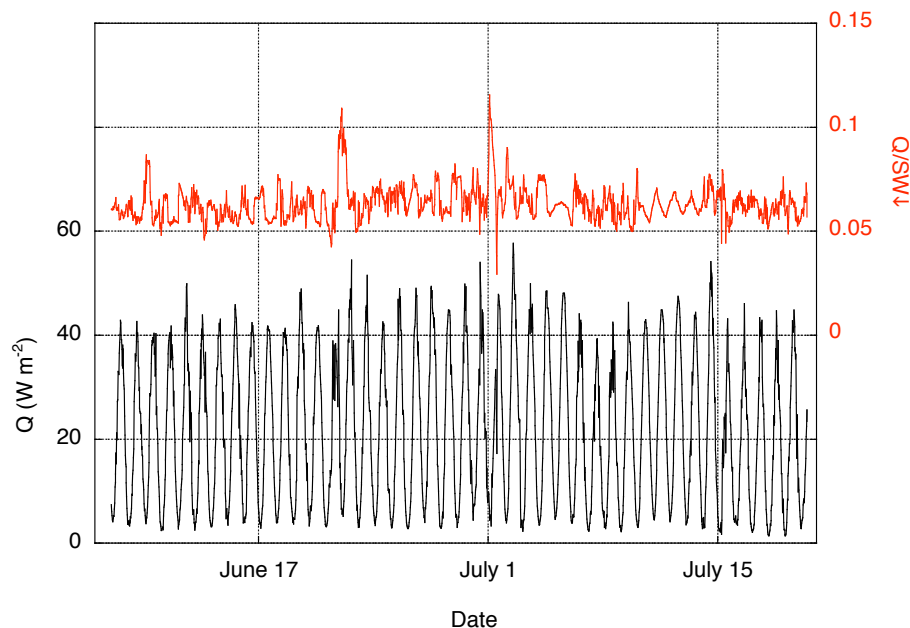


Fig. 4. Amount of radiation absorbed at least 0.5 cm below the surface Q (W m^{-2}) in black, and its fraction of incoming solar radiation SW_l in red.

[Title Page](#)[Abstract](#)[Introduction](#)[Conclusions](#)[References](#)[Tables](#)[Figures](#)[I◀](#)[▶I](#)[◀](#)[▶](#)[Back](#)[Close](#)[Full Screen / Esc](#)[Printer-friendly Version](#)[Interactive Discussion](#)

**Radiation penetration
at Summit, Greenland**

P. Kuipers Munneke et al.

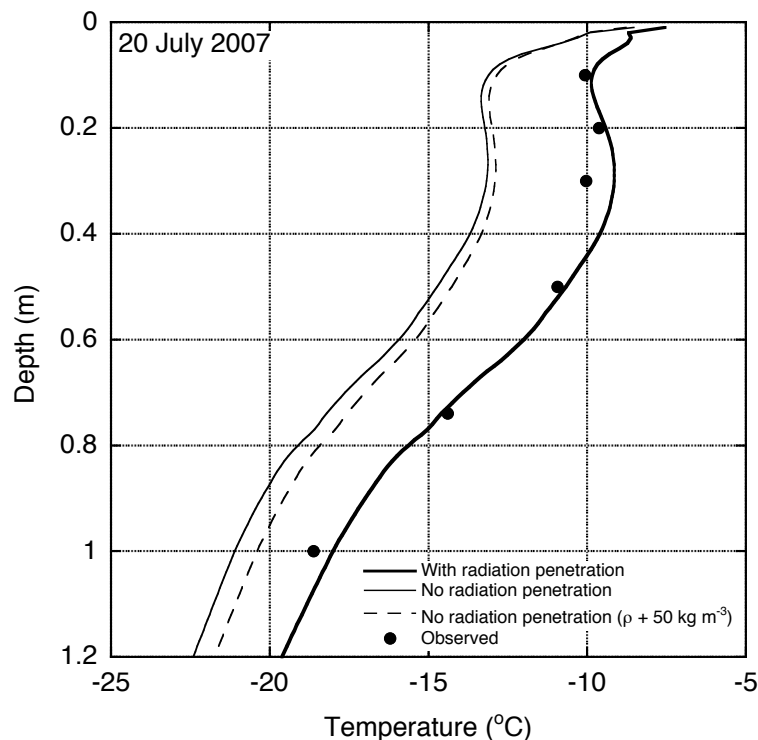


Fig. 5. Temperature profiles at the end of the 42-day experiment, measured (solid dots) and modeled, with radiation penetration (thick solid line), without radiation penetration (thin solid line) and without radiation penetration and higher snow density (+50 kg m⁻³).

[Title Page](#)[Abstract](#)[Introduction](#)[Conclusions](#)[References](#)[Tables](#)[Figures](#)[I◀](#)[▶I](#)[◀](#)[▶](#)[Back](#)[Close](#)[Full Screen / Esc](#)[Printer-friendly Version](#)[Interactive Discussion](#)

**Radiation penetration
at Summit, Greenland**

P. Kuipers Munneke et al.

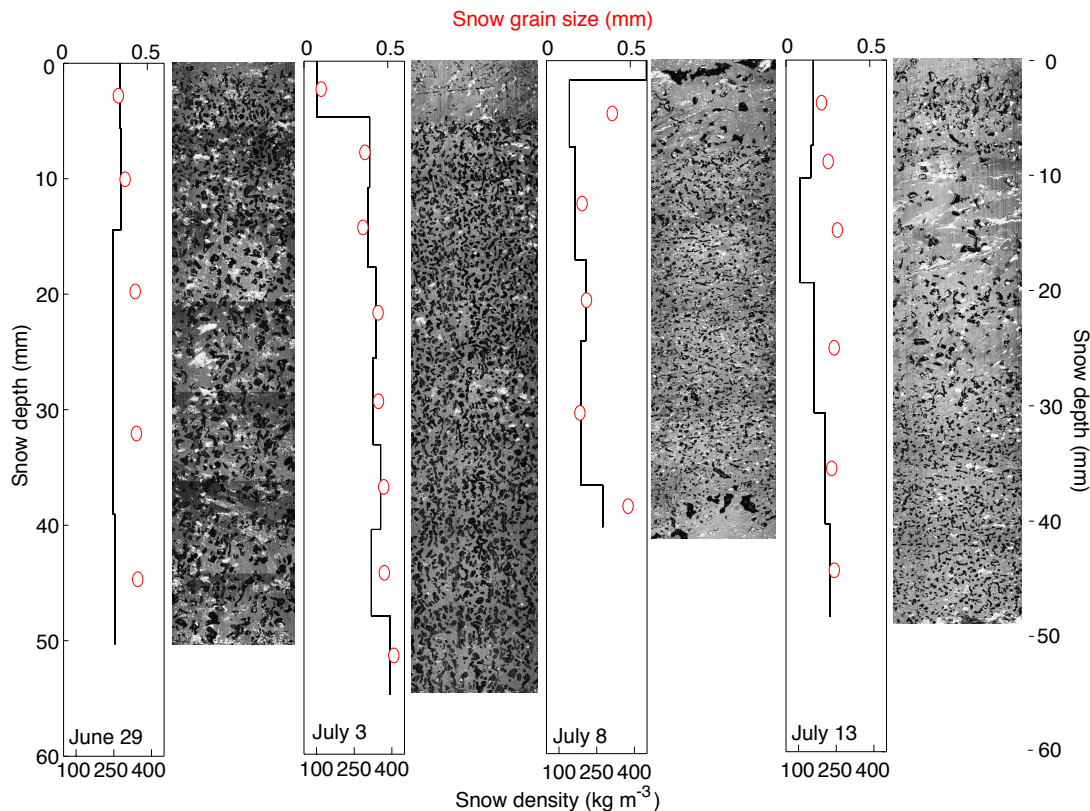


Fig. 6. Profiles of snow density (black lines, lower horizontal axis) and snow grain size (red circles, upper horizontal axis), from stereographical analysis of snow samples. The dates on which the snow samples were collected are displayed in each frame.

[Title Page](#)[Abstract](#)[Introduction](#)[Conclusions](#)[References](#)[Tables](#)[Figures](#)[I◀](#)[▶I](#)[◀](#)[▶](#)[Back](#)[Close](#)[Full Screen / Esc](#)[Printer-friendly Version](#)[Interactive Discussion](#)

Radiation penetration
at Summit, Greenland

P. Kuipers Munneke et al.

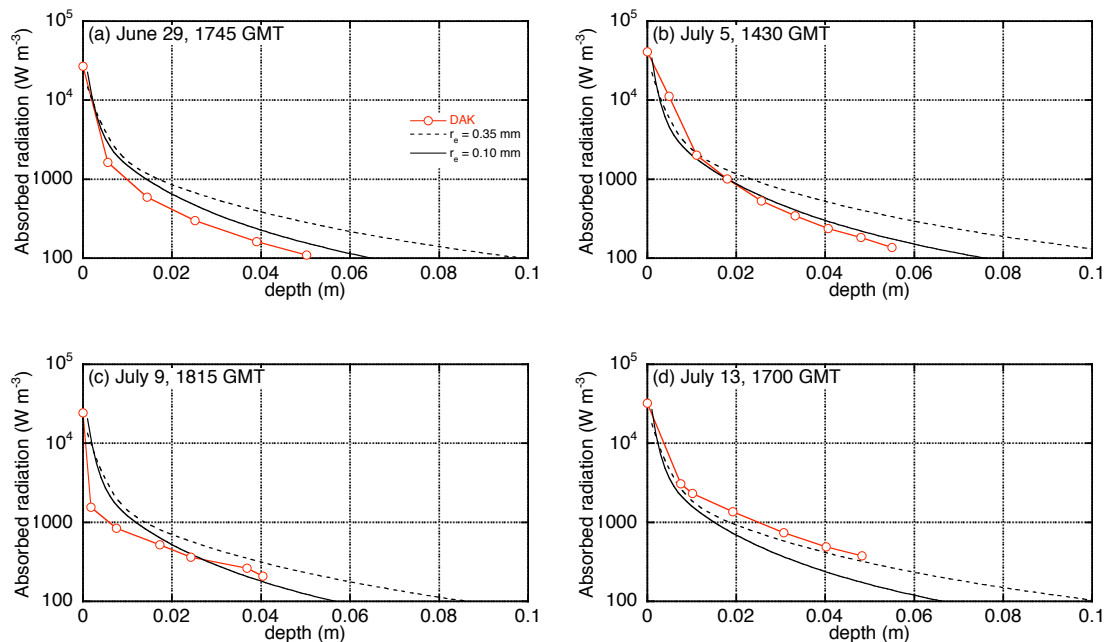


Fig. 7. Profiles of absorbed radiation in W m^{-2} per m. Red circles are calculations with the radiative transfer model DAK, whereas black lines are profiles from the two-stream model for snow grain radius $100 \mu\text{m}$ (solid) and $350 \mu\text{m}$ (dashed).

Title Page

Abstract

Introduction

Conclusions

References

Tables

Figures

I◀

▶I

◀

▶

Back

Close

Full Screen / Esc

Printer-friendly Version

Interactive Discussion



Radiation penetration at Summit, Greenland

P. Kuipers Munneke et al.

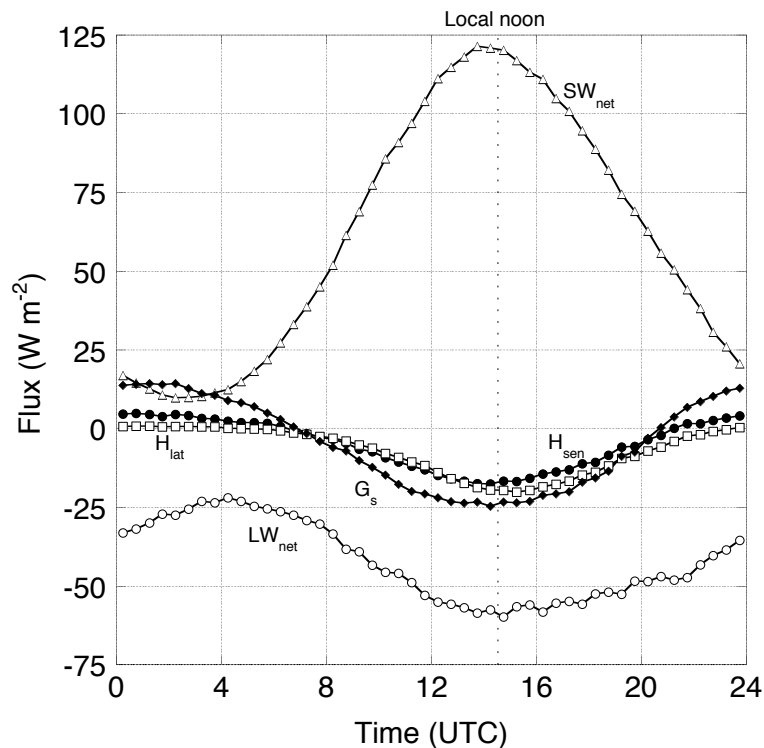


Fig. 8. Average diurnal cycle of the surface energy balance components, in W m^{-2} . Shown are net solar radiation (triangles), net longwave radiation (open circles), turbulent sensible (solid circles) and latent (open squares) heat fluxes, and subsurface heat flux (solid diamonds). The dashed vertical line represents the local noon at 14:33 UTC.

[Title Page](#)
[Abstract](#)
[Introduction](#)
[Conclusions](#)
[References](#)
[Tables](#)
[Figures](#)
[I◀](#)
[▶I](#)
[◀](#)
[▶](#)
[Back](#)
[Close](#)
[Full Screen / Esc](#)
[Printer-friendly Version](#)
[Interactive Discussion](#)
